Oil & Natural Gas Technology

Quarterly Progress Report
(October - December 2010)

Mechanisms Leading to Co-Existence of Gas and Hydrate in Ocean Sediments

Submitted by:
The University of Texas at Austin
1 University Station C0300
Austin, TX 78712-0228

February 2, 2011

NETL

Office of Fossil Energy

MECHANISMS LEADING TO CO-EXISTENCE OF GAS AND HYDRATE IN
OCEAN SEDIMENTS

CONTRACT NO. DE-FC26-06NT43067

QUARTERLY PROGRESS REPORT
Reporting Period: 1 Oct 10 – 31 Dec 10

Prepared by

Steven L. Bryant
Department of Petroleum and Geosystems Engineering
The University of Texas at Austin
1 University Station   C0300
Austin, TX   78712-0228
Phone: (512) 471 3250
Email: steven_bryant@mail.utexas.edu

Ruben Juanes
Department of Civil and Environmental Engineering
Massachusetts Institute of Technology
77 Massachusetts Avenue, Room 48-319
Cambridge, MA 02139
Phone: (617)253-7191
Email: juanes@mit.edu

Summary

We have systematically refined an earlier version of a "box model" that determines the masses of methane and water that are required to maintain constant pressure during the conversion of a gas accumulation to hydrate. This calculation is useful for modeling sub-permafrost hydrate accumulation because it constrains one of several independent transport processes (supply of methane and water, transport of heat of fusion and transport of salinity) that can limit hydrate formation from a gas phase. The model takes as input the initial saturation of gas phase at a given location in a sediment and a user-specified ratio of the volumes of gas and brine phases that enter that location. The output of the model is the final hydrate saturation.

The model can be used in a hindcasting mode to constrain the likely ratio of gas and brine volumes that entered the sediment, given a likely value of initial gas saturation and the observed value of modern hydrate saturation. Alternatively, if the likely ratio of gas and brine volumes can be independently estimated, then the model can be used to forecast hydrate saturation distributions from an initial gas saturation distribution.

To address the latter alternative, we have developed a pore-level model of hydrate growth at gas-brine interfaces. For simplicity this model assumes that all hydrate films are mechanically robust; the case of films breaking when subject to a pressure difference has been described in previous reports. Depending on whether the rate of supply of water to the hydrate interface is slow or fast relative to the rate of hydrate growth, the model predicts a one-to-one replacement of gas-filled pores by hydrate-filled pores (slow water supply), or a mixture of water-filled pores enclosed by hydrate shells (fast water supply). The volume of phases in realistic granular material is readily accessible from our level-set method simulation of drainage and imbibition. Thus these two limiting cases can constrain the ratio of volumes of gas and water that enter the domain. These ratios can then be used to predict modern hydrate saturations, and these predictions will be described in future reports.

Activities in This Reporting Period

Task 8.0 - Modeling methane transport at the bed scale

Subtask 8.1 Application of bed-scale model to sub-permafrost hydrate accumulations

OVERVIEW

We have systematically refined an earlier version of a "box model" that determines the masses of methane and water that are required to maintain constant pressure during the conversion of a gas accumulation to hydrate. This calculation is critical for modeling sub-permafrost hydrate accumulation because for typical conditions forming an incremental volume of hydrate results in a net decrease in volume occupied by gas, brine and hydrate phases. In nature, this void will be filled either by sediment compaction (reducing pore volume by reducing bulk volume via grain rearrangement) or by migration of gas and/or brine phases into the hydrate stability zone. There are obvious limits to the extent of compaction, and thus we assume that only fluid migration fills the incipient void during hydrate formation. The model takes as input the initial saturation of gas phase at a given location in a sediment and a user-specified ratio of the volumes of gas and brine phases that enter that location. The output of the model is the final hydrate saturation.

The model can be used to constrain the likely ratio of gas and brine volumes that entered the sediment, given a likely value of initial gas saturation and the observed value of modern hydrate saturation. Alternatively, if the likely ratio of gas and brine volumes can be independently constrained, then the model can be used to predict hydrate saturation distributions from an initial gas saturation distribution. As discussed in previous reports, sedimentological variation with depth can lead to disconnection of the gas phase within the accumulation, and the model predicts large variations in hydrate saturation even where gas saturations were originally constant.

MODEL DEVELOPMENT

A simple box model is used to compute the volume change as hydrate forms. The box (with a volume V_0) is originally filled by methane and water (Figure 1a). The initial gas/water saturations are fixed, and $S_w = 1 - S_g$ and no hydrate is present initially. An

increment of hydrate δS_h forms at the interface between gas and water phase (Figure 1b). We assume the hydrate increment is the result of stoichiometric conversion of the corresponding increments of methane and water, δS_g and δS_w. The relationship between the saturation increments depends on the densities of the phases. Temperature and pressure are assumed appropriate for hydrate formation and almost constant during hydrate formation process. Therefore, gas and water phase have constant density during hydrate formation and thus volume change. Under conditions typical of sub-permafrost, the hydrate formation results in system volume reduction, as shown by the blank box at the right hand side of the aqueous phase in Figure 1(b). Such reduction is because the hydrate (density about 910 kg/m^3) occupies less volume than the converted water (density 1010 kg/m^3)and gas (density 50 to 100 kg/m^3). Mathematically we have:

$$\delta S_w + \delta S_w = \delta S_h + \delta V \tag{1.1}$$

Since we assumed a constant pressure and temperature during the hydrate formation process, two different consequences will emerge depending on whether we have a closed or open system .
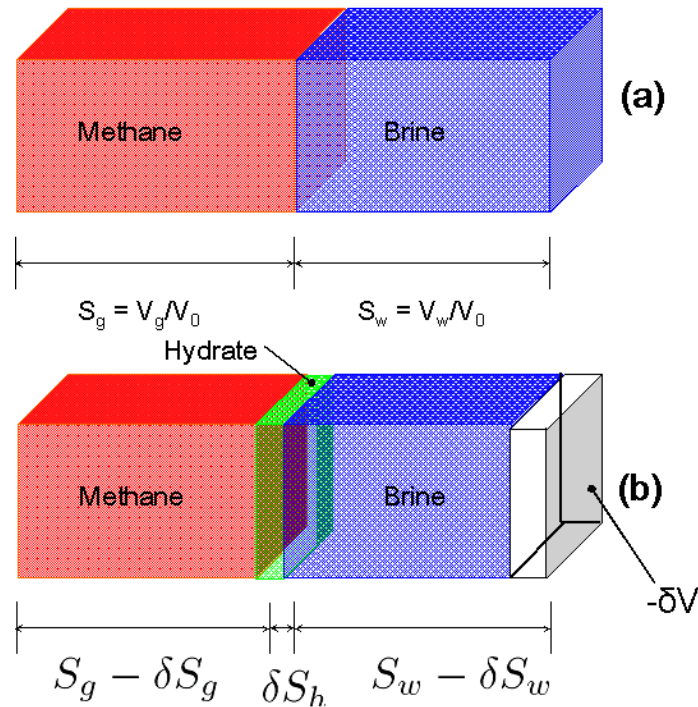

Figure 1- The box model to compute the volume change due to hydrate formation. (a) The initial gas/water saturations are fixed, and $S_w = 1 - S_g$. No hydrate is present initially. (b) An increment of hydrate δS_h forms at the interface between gas and water phases. The volume increment δV is negative for phase densities typical of sub-permafrost conditions.

For a closed system (no fluid transport in or out of the system) the only way to keep the pressure and temperature constant is through system volume change, i.e. the total volume of the system will shrink. **Figure 2**a shows a cylinder with a movable piston initially containing methane and water. For simplicity water is assumed to be fresh; therefore, salinity build-up will not limit the hydrate formation (limiting case). Hydrate starts growing at the interface of methane and water (**Figure 2**b) and will keep forming until one of the phases (gaseous or aqueous) will be fully consumed.
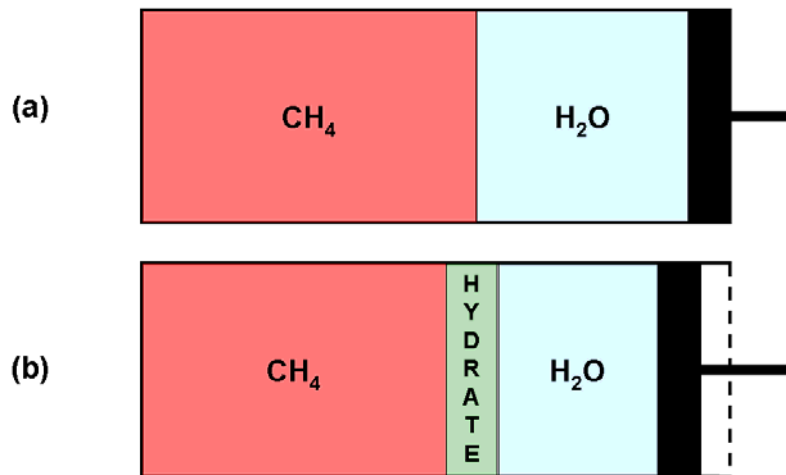
Figure 2- (a) shows the initial state of a closed system; (b) shows the system after an increment of hydrate formation

Therefore, we will end up with methane and methane hydrate if we have excess gas (**Figure 3**a). On the other hand, the system will end up having water and methane hydrate if we have excess water (**Figure 3**b) Note that the pressure is kept constant with the movable piston, while instantaneous heat exchange is assumed to maintain the temperature constant.
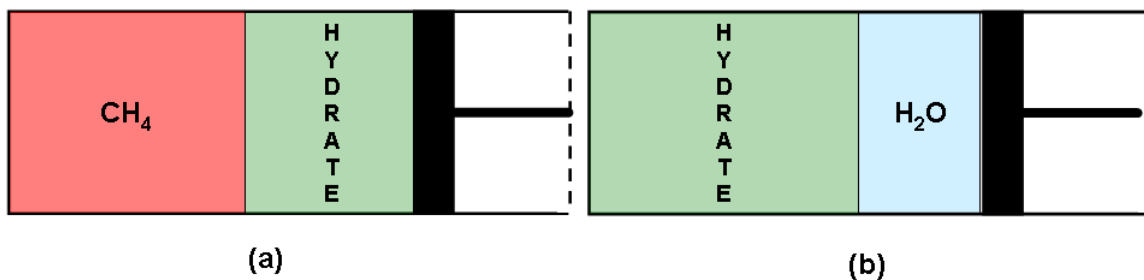
Figure 3- (a) Final state of the system if methane gas (CH_4) is in excess; (b) Final state of the system when water (H_2O) is in excess.

It can be shown that the volume-change (which is compensated by piston movement) in each case is as the following:

➢ Gas phase in excess:

$$\frac{\Delta V}{V} = S_w \left(\frac{\rho_w}{\rho_h} \frac{M_g + N M_w}{N M_w} - \left(1 + \frac{\rho_w}{\rho_g} \frac{M_g}{N M_w} \right) \right) \tag{1.2}$$

➢ Water phase in excess:

$$\frac{\Delta V}{V} = S_g \left(\frac{\rho_g}{\rho_h} \frac{M_g + N M_w}{M_g} - \left(1 + \frac{\rho_g}{\rho_w} \frac{N M_w}{M_g} \right) \right) \tag{1.3}$$

On the other hand, in natural situations we mostly have open systems rather than closed systems, so that it is open to fluid flow. Figure 4 shows an open system with an initial state of water and methane content as n_{CH4} moles of methane and n_{H2O} moles of water.
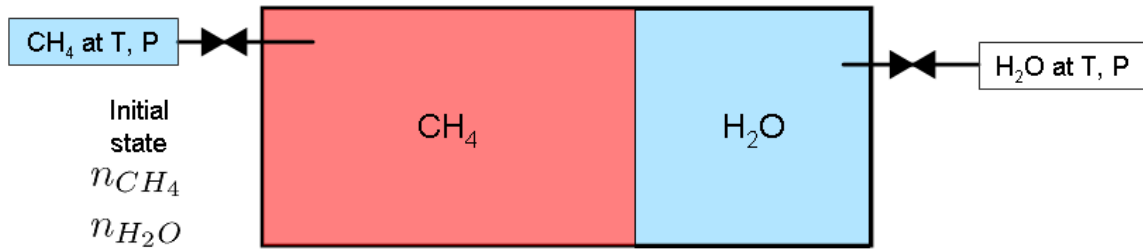

Figure 4- Open system: CH_4 can enter, H_2O can enter so that T, P constant.

Pressure and temperature is assumed constant and appropriate for hydrate formation. In addition, both water and methane are allowed to enter the system to compensate for the volume reduction while hydrate formation and thus maintain the pressure. Hydrate will keep forming until one or both of the ingredients (methane, water or both) are fully consumed. Once the hydrate formation stops, two limiting cases can be considered in terms of the amount of water and methane transported into the system:

➢ Limiting case 1: Only gas has entered the system ($\Delta n_{H2O} = 0$)

In this case, hydrate will form until all the water initially present in the system is consumed. **Figure 5** shows the final state of the system for this limiting case, where Δn_{H2O} is the total number of moles of water entered the system.
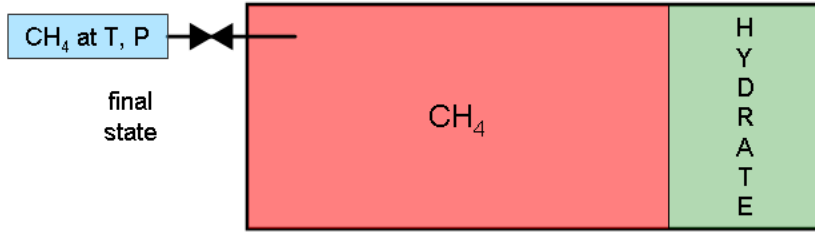
Figure 5- Final state of the open system when no water enters the open control volume from outside ($\Delta n_{H2O} = 0$)

➢ Limiting case 2: Only waters has entered the system ($\Delta n_{CH4} = 0$)

In this case, hydrate will form until all the initially present gas in the system is consumed. **Figure 6** shows the final state of the system for this limiting case, where Δn_{CH4} is the total number of moles of methane entered the system.
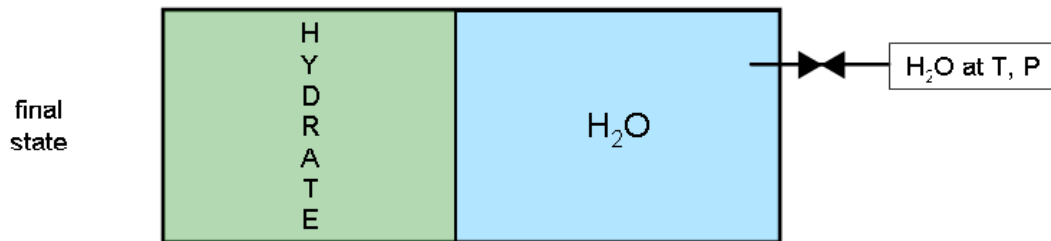

Figure 6- Final state of the open system when no water enters the open control volume from outside ($\Delta n_{CH4} = 0$)

A natural system is somewhere between the above limiting cases but neglecting the salinity effect (assuming fresh water) hydrate will keep forming until we run out of either methane or water in the system. Therefore, we will end up with a system having either methane and hydrate only or water and hydrate only. One can imagine a case in which the number of moles of gas and water entering the system are at the right proportion at which the system ends up having hydrate only. Although the probability that this special case takes place is infinitesimal, it gives us a reference point to determine the two general cases of excess water or excess gas. The special case mentioned takes place only if the total amount of gas ($n_{CH4} + \Delta n_{CH4}$) and the total amount of water ($n_{H2O} + \Delta n_{H2O}$) are stoichiometric:

$$6(n_{CH4} + \Delta n_{CH4}) = (n_{H2O} + \Delta n_{H2O}) \tag{1.4}$$

7

Equation 1.4 implies critical ratio of the amounts of CH_4 and H_2O that entered. Therefore, one can define a critical molar ratio of gas entering the system as:

$$R_{s,n} = \frac{\Delta n_g}{\Delta n_g + \Delta n_w} \quad \text{where} \quad 6(n_{CH4} + \Delta n_{CH4}) = (n_{H2O} + \Delta n_{H2O}) \tag{1.5}$$

For phase volume ratios on either side of this special point, we have two general cases: (1) excess gas or (2) excess water.

In the case of excess gas the total number of gas moles ($n_{CH4} + \Delta n_{CH4}$) is more than the stoichiometric requirements and thus:

$$R_{s,n} < R_n = \frac{\Delta n_g}{\Delta n_g + \Delta n_w} \leq 1 \tag{1.6}$$

The resulting hydrate saturation for each value of R_n can be calculated solving for the following system of equations

$$
\begin{cases}
V_g = (n_g + \Delta n_g - \dfrac{n_w}{N} - \dfrac{1-R_n}{NR_n} \Delta n_g)(\dfrac{MW_g}{\rho_g}) \\[2ex]
V_h = (\dfrac{n_w}{N} + \dfrac{1-R_n}{NR_n} \Delta n_g)(\dfrac{MW_h}{\rho_h}) \\[2ex]
V_g + V_h = V_{tot}
\end{cases}
\tag{1.7}
$$

Once the gas and hydrate volume, V_g and V_h, are known then the final hydrate saturation can be easily calculated as $S_h = \dfrac{V_h}{V_{tot}}$. In this case the system will end up having hydrate and gas only.

On the other hand, for the case of excess water the total number of water moles will be more than stoichiometric and thus:

$$0 \leq R_n = \frac{\Delta n_g}{\Delta n_g + \Delta n_w} < R_{s,n} \tag{1.8}$$

Similarly, to calculate the hydrate saturation one can solve the following system of equations and calculate the hydrate saturation as $S_h = \dfrac{V_h}{V_{tot}}$.

$$\begin{cases} V_w = (n_w + \dfrac{1-R_n}{R_n}\Delta n_g - N(n_g + \Delta n_g))(\dfrac{MW_w}{\rho_w}) \\[3mm] V_h = (n_g + \Delta n_g)(\dfrac{MW_h}{\rho_h}) \\[3mm] V_w + V_h = V_{tot} \end{cases} \qquad (1.9)$$

Similar to the molar ratio of gas entering the system (R_n), a volumetric ratio of gas entering the system as (R_v) is defined as:

$$R_v = \frac{\Delta V_g}{\Delta V_g + \Delta V_w} = \frac{\Delta n_g(\dfrac{MW_g}{\rho_g})}{\Delta n_g(\dfrac{MW_g}{\rho_g}) + \Delta n_w(\dfrac{MW_w}{\rho_w})} \qquad (1.10)$$

$$\Rightarrow R_v = \frac{\Delta n_g}{\Delta n_g + \Delta n_w(\dfrac{MW_w}{MW_g})(\dfrac{\rho_g}{\rho_w})} \qquad (1.11)$$

Volumetric ratios, R_v, will be useful specially if we want to apply the relative permeability curves for which the volumetric quantities are being used.

MODEL IMPLICATIONS

Using the formulations above one can calculate the resulting hydrate saturation in addition to gas/water saturation for different values of R_n or R_v for a given initial gas/water saturation. For instance, **Figure 7** shows the resulting hydrate saturation versus R_n for a control volume 40% saturated with water and 60% saturated with gas initially. For this initial state, for values of R_n less than 0.2 we end up having hydrate and water only (excess water) and for R_n greater than 0.2 we end up having hydrate and gas only (excess gas).

Doing the calculations based on R_v rather than R_n, one can easily determine the final hydrate saturation based on the ratio of phase volumes (water to gas) entering the system (assuming the initial state of the system is known). **Figure 8** shows the resulting hydrate saturation from the same control volume as in Figure 7 as a function of R_v instead of R_n. The same curve could be calculated plotted for different initial phase saturations. **Figure 9** shows the corresponding curves for a set of initial gas/water saturation within the control volume. On each of these curve there is a single point at which $S_h = 1$,

meaning that the amount of water and gas entering the control volume where at the exact right proportion for to get fully converted into hydrate. We denote the R_v at this specific point as R_v^*. For instance R_v^* is about 0.8 for a control volume with initial water saturation of $S_{wi} = 0.4$ (**Figure 8**).
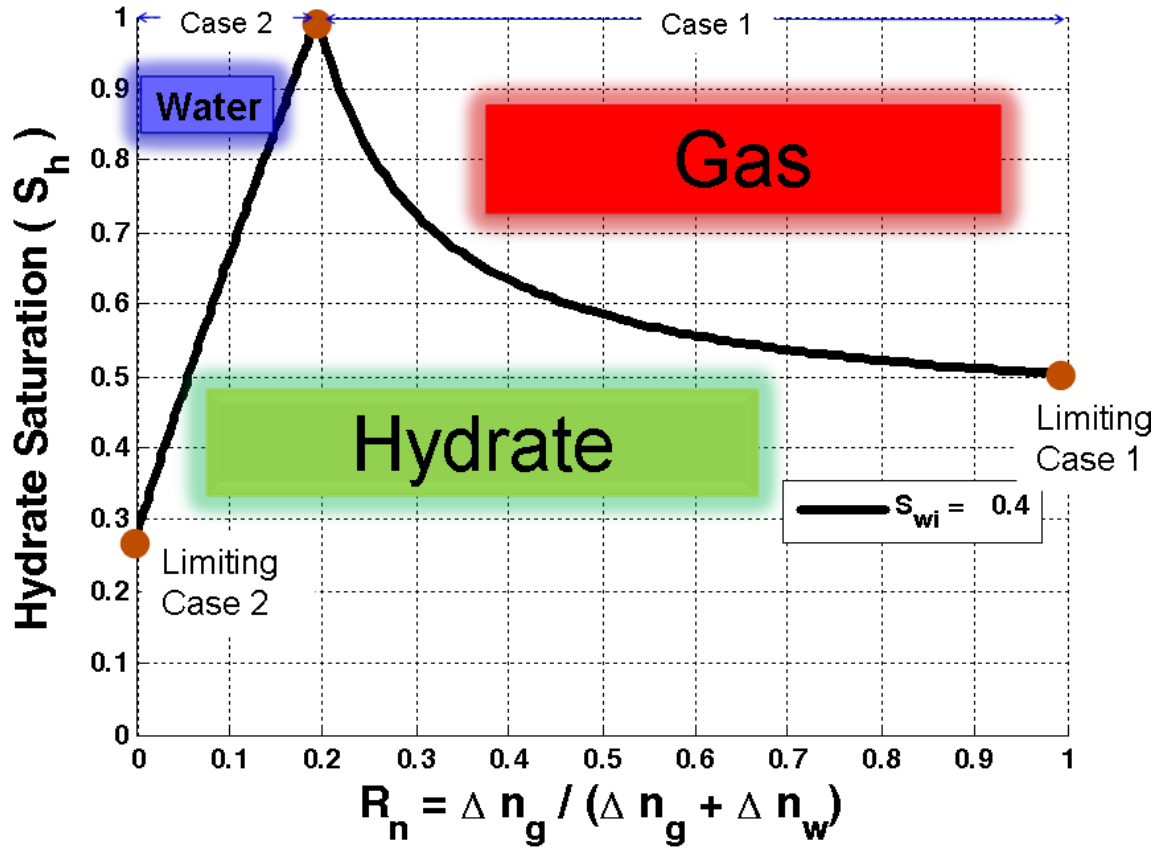

Figure 7- Plot of hydrate saturation versus R_n for a control volume having 40% water and 60% gas initially.
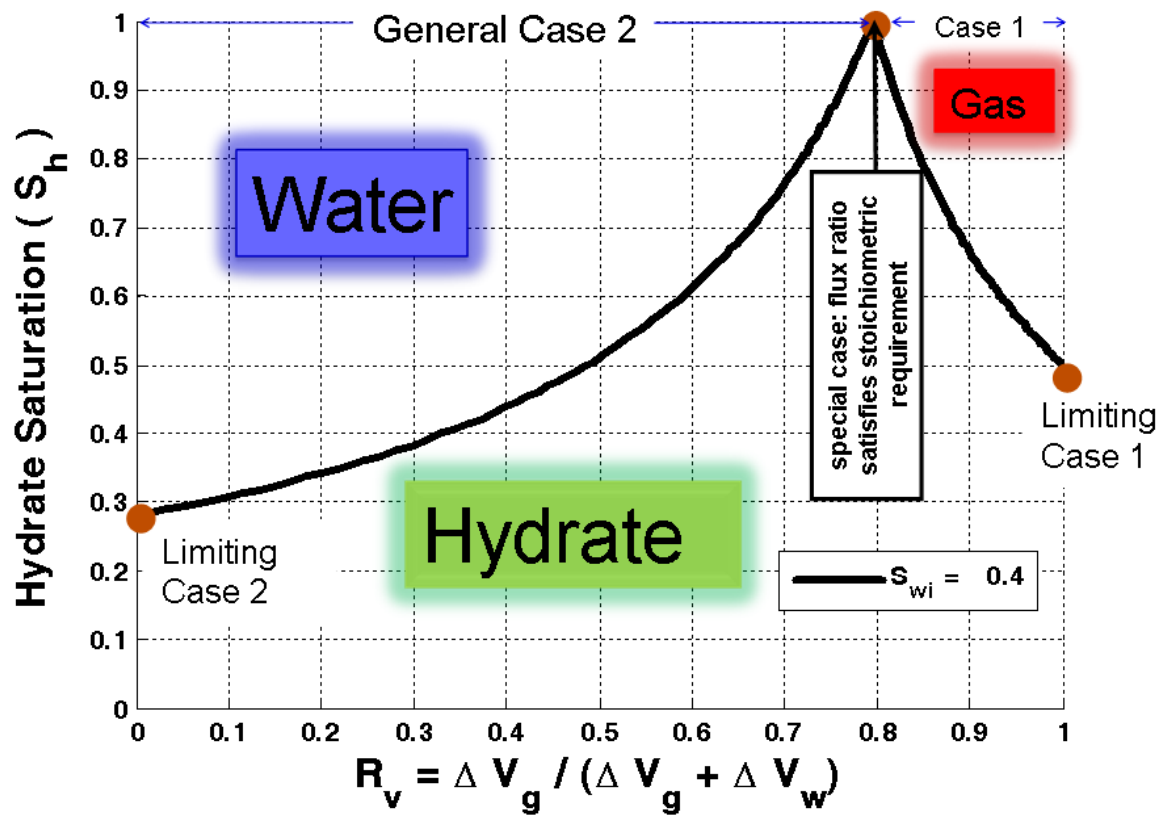
Figure 8- Plot of hydrate saturation versus R_v for a control volume having 40% water and 60% gas initially.
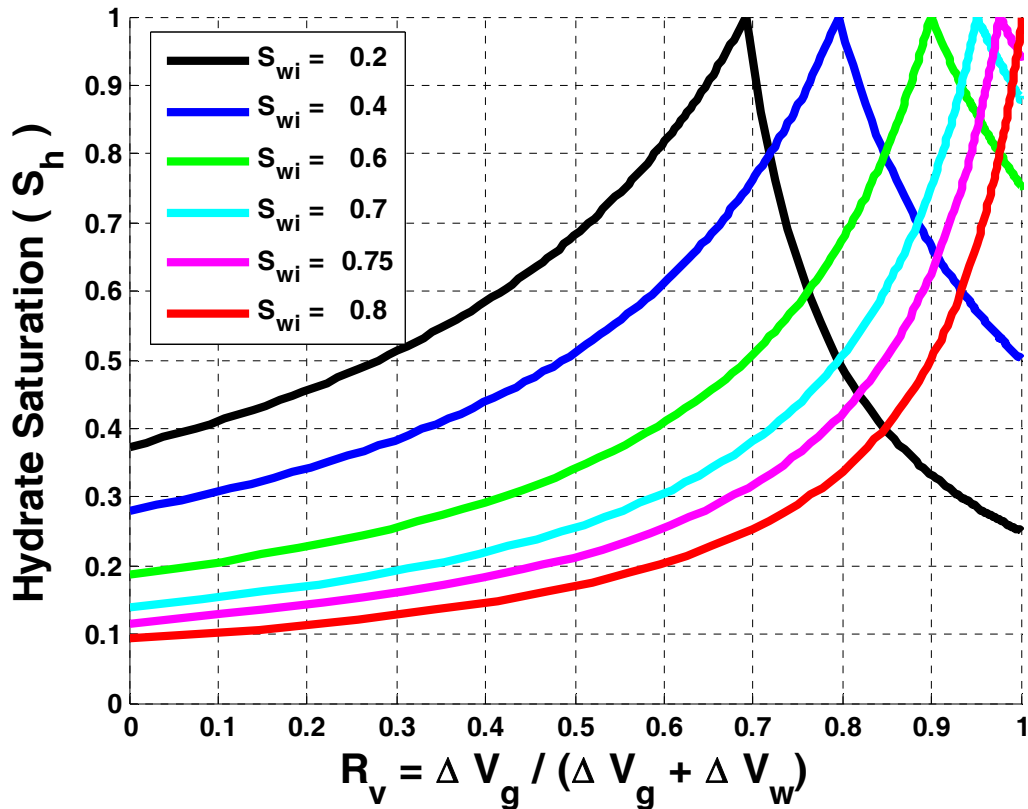
Figure 9- Plot of hydrate saturation versus R_v for a control volume with under different initial fluid saturations

Therefore, if the initial gas/water saturation distribution is known, assuming that gas hydrate starts forming from above, and knowing the values of R_v or R_n we can estimate the resulting hydrate saturation profile from the initial gas/water saturation distribution. Similarly, the hydrate saturation could be related to the amount (volume) of gas entering the control volume. **Figure 10** shows two lines (one for excess gas and one for excess water) relating the resulting hydrate saturation to the amount of gas entered the control volume. Note that the volume of the control volume was assumed to be unity and the initial water and gas saturation was 0.4 and 0.6 respectively. It is seen that considerable amount of gas (compared to the volume of control volume) might move into the control volume.
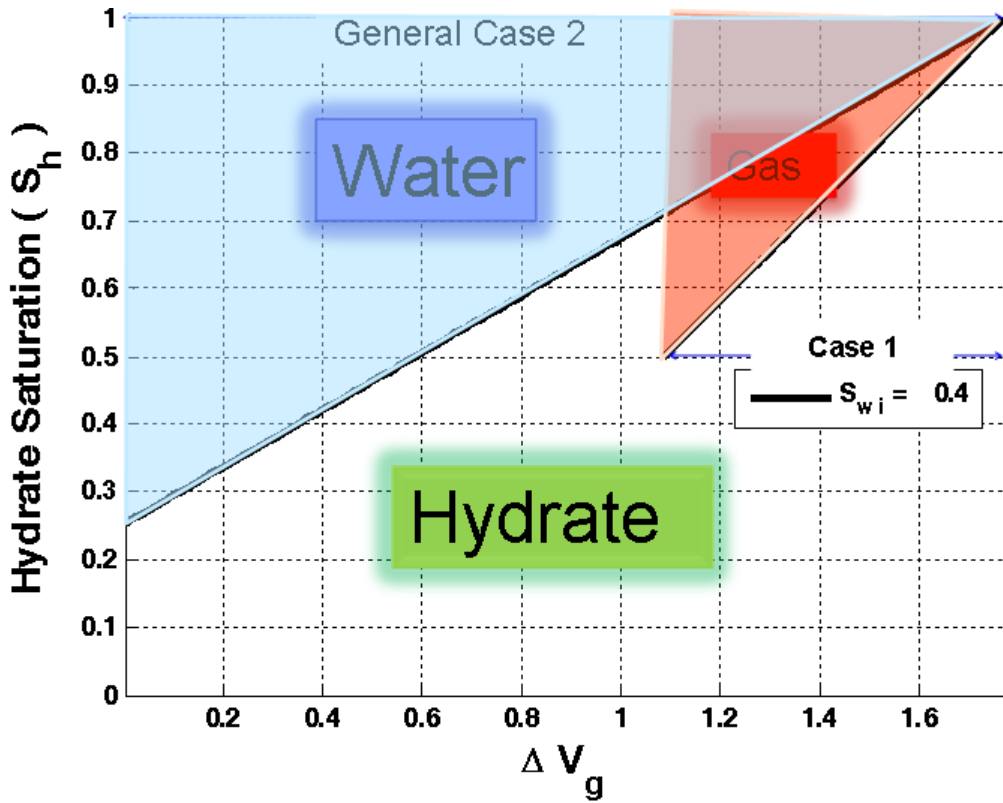
Figure 10- Hydrate saturation versus the gas volume entering the control volume with initial water saturation of 0.4 ($S_g = 0.6$). Note that the control volume is assumed to have unit a volume. For cases of excess gas use the right-hand side line and for excess water cases use the left-hand side line.

The same graph can be plotted for hydrate saturation versus water volume moving into the control volume.
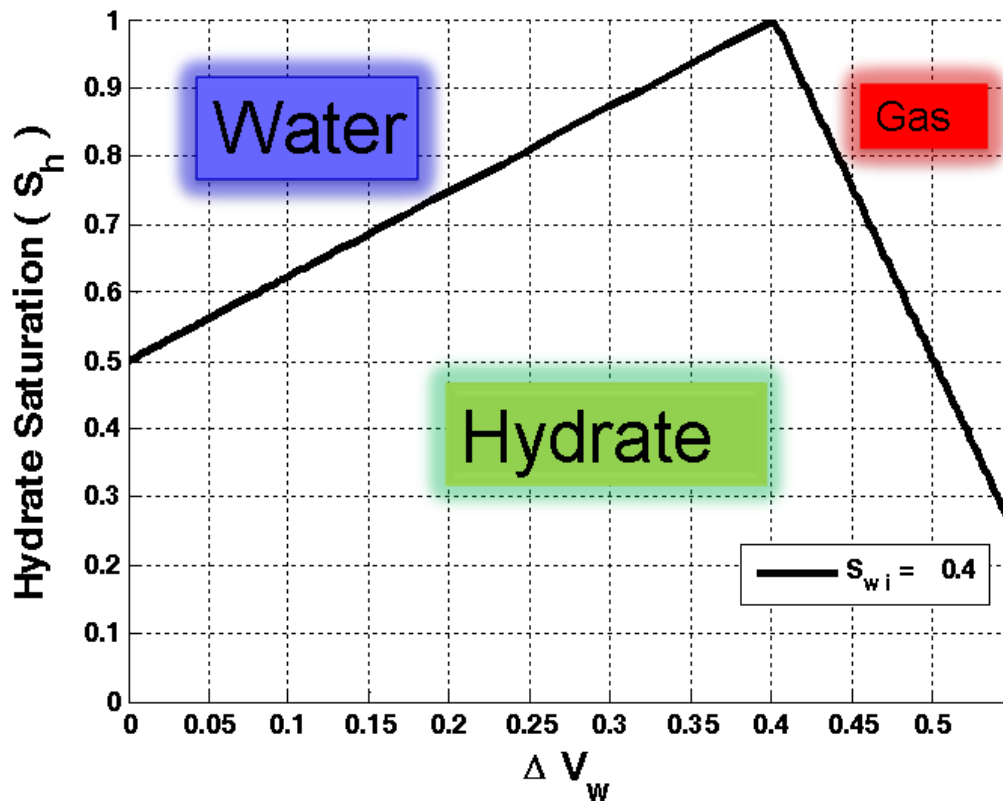
Figure 11- Hydrate saturation versus the water volume entering the control volume with initial water saturation of 0.4 ($S_g = 0.6$). Note that the control volume is assumed to have unit a volume. For cases of excess gas use the right-hand side line and for excess water cases use the left-hand side line.

To illustrate the amount of fluid needed to be transported into hydrate-bearing sediments, total fluid volume ($\Delta V_w + \Delta V_g$) is plotted versus observed hydrate saturation for different initial conditions in Figure 12. Plots have been provided for cases of excess water and gas separately. It is seen that these graphs turn out to be a set of straight lines that partially overlap each other. More importantly the plots show that for high hydrate saturations (like that observed in Mt. Elbert stratigraphic test well) the amount of fluid transporting into the hydrate-bearing zone is considerably high, ranging between 1.3 to almost twice as much as the initial fluid (water + gas) present.
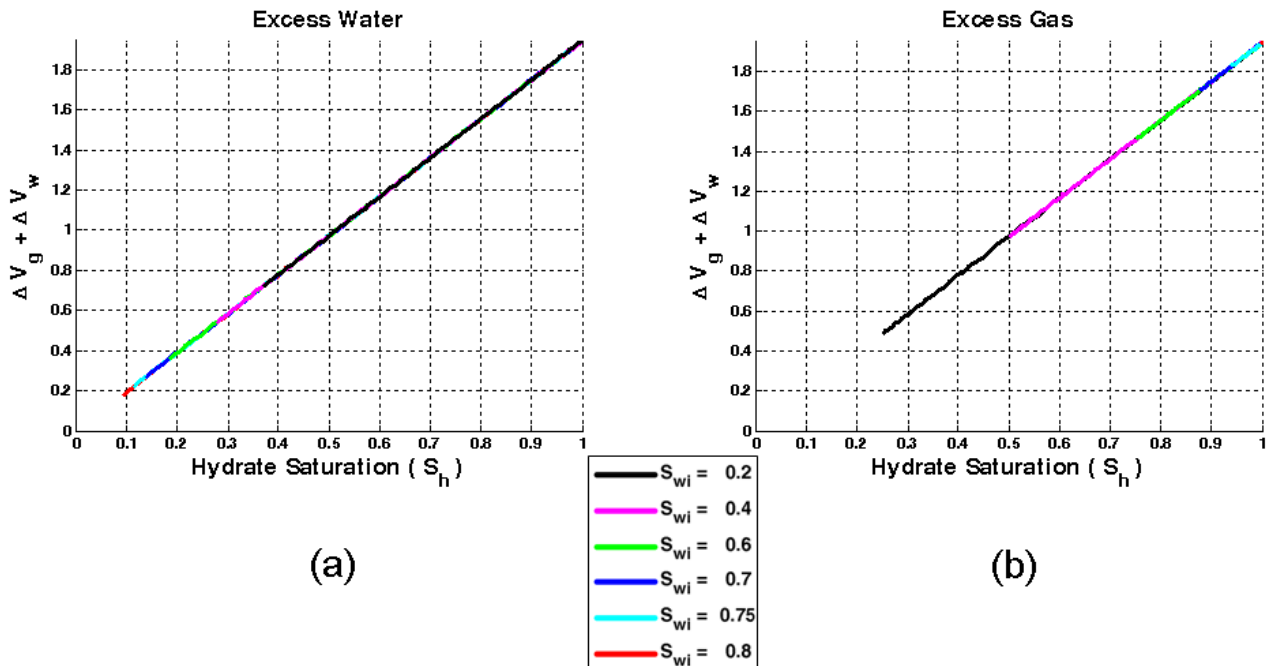
Figure 12- total fluid volume versus observed hydrate saturation in a control volume with unit volume. (a) shows the case of excess water when we only observed water and hydrate in the control volume and (b) shows the excess gas case where we observe gas and hydrate in the control volume.

SUMMARY

The model described above determined the range of possible hydrate saturations that can result from converting a given gas saturation. It does not however allow *a priori* prediction of what hydrate saturation will occur unless an independent assessment of the relative rates of brine phase and gas phase supply to the hydrate stability zone is available. In the next section we develop a framework for assessing these relative rates, using pore scale models previously developed in this project.

Hydrate saturation prediction from pore scale --- the effect of gas saturation footprint

OVERVIEW

In hydrate-bearing sediments in several provinces around the world, many factors support the hypothesis that modern hydrate is the result of converting an earlier accumulation of gas. The conversion took place as the base of the gas hydrate stability zone (BGHSZ) descended over geologic time, either as sea level rose (above ocean sediments) or air temperature decreased (at the surface above Arctic sediments).

The overall hydrate distribution at the field scale resulting from this type of conversion is determined by many factors. An important one is the hydrate formation in the pore-scale, which determines the hydrate saturation at each layer of the reservoir. Another factor is the need to redistribute the free gas in the vertical direction, driven by the decline in pressure caused by hydrate formation discussed in the previous section of this report. Here we propose two pore-scale models that would yield the maximal and minimal hydrate saturation in the porous medium. We illustrate the model with a 2D porous medium, for the purpose of better visualization and demonstration. The extension from 2D to 3D is not a difficult task, and the results will be available in subsequent reports.

We assume the following scenario for hydrate formation at the pore scale. The steps are discussed in more detail with schematics in subsequent sections.

1. The gas phase (pure methane) and brine phase (salinity assumed constant) are at capillary equilibrium, so that gas/brine interfaces are static. Our model also assumes that both methane and brine are connecting to the bulk volume, and thus none of them would be exhausted.

2. The first layer of hydrate crystal forms along the interface between methane and water when the local temperature and pressure reach the phase equilibrium boundary (the hydrate-water/gas-water boundary). 'Water' and 'brine', 'gas' and 'methane' are used interchangeably in this section.

3. Forming a layer of hydrate reduces the gaseous phase volume more than the aqueous phase, since volumetrically hydrate formation consumes more methane than water at typical hydrate stability conditions (P = 5 to 10 MPa, T = 3 to 10 C). Therefore, hydrate preferentially grows into the gaseous phase. In this fashion a layer of hydrate appears between gas and water, and the gas/brine interface is replaced by a gas/hydrate interface, a thin hydrate layer, and a hydrate/brine interface.

4. Continued growth of hydrate requires water to migrate from the water phase in the sediment through microscopic defects (e.g. boundaries at crystal defects within the hydrate, grain surface roughness, etc.) to the gas/hydrate interface.

5. The total vacancy (reduction in gas volume + reduction in brine volume) generated when an incremental volume of hydrate forms is filled by brine phase. Depending upon the connectivity of the brine phase (between the interface where hydrate is forming and the bulk phase of formation brine) and, more critically, upon the rate at which water can migrate through the existing hydrate in step (4), the rate of this filling may be faster or slower than the rate of hydrate formation at the interface.

In this model, hydrate saturation that accumulates at the base of the gas hydrate stability zone can vary between maximal and minimal values. If the water supply rate is much smaller than the hydrate formation rate, hydrate saturation will reach a maximal

value. On the other hand if the water supply rate is much larger than the hydrate formation rate, hydrate saturation will reach the minimal value. **Appendix A** provides an estimate of the water supply rate through the hydrate layer. The purpose of this section is to identify the two limiting cases, and give an insight into the hydrate formation in the porous medium.

Limiting case #1: water supply rate much smaller than hydrate formation rate
In this limiting case hydrate formation is controlled by the water availability. Thus the water supply rate controls the rate of hydrate formation. Figure 13 demonstrates this case in a small 2D domain. The gray disks are sand grains, blue regions correspond to the brine phase, green region is gas phase, and the red region is the hydrate. The initial wetting and nonwetting phase distribution (Figure 13A) is obtained by simulating a drainage endpoint with our Level Set Method Progressive Quasi-Static algorithm (LSMPQS). The initial nucleation happens at the fluid-fluid interface, which consumes both water and gas. The hydrate layer cannot form as a single crystal, and the microscopic defects within the layer of crystals allow water to imbibe through the hydrate layer and form a thin layer of water at the hydrate surface (Figure 13B the zoom-in figure, notice the thin water layer (blue) on the gaseous phase (green)). Since hydrate formation is rapid compared to water supply, this water layer is quickly converted into hydrate. This further reduces the gaseous phase pressure (Figure 13B and C) and water again imbibes to the gas-hydrate interface. During this process, we assume that the curvature of hydrate layer maintains the curvature of capillary-equilibrium between gas and water, and therefore the hydrate invasion into the gaseous phase can be approximated as the imbibition process (the curves in Figure 13 are computed by LSMPQS simulation). This stage of the hydrate formation (Figure 13B and C) is referred to as the stage 1.

A. The initial methane (green) and water (blue) distribution in a porous medium (gray disks represent the grains). The distribution is in capillary equilibrium (satisfies Young-Laplace equation), obtained from the drainage endpoint by the LSMPQS simulation.
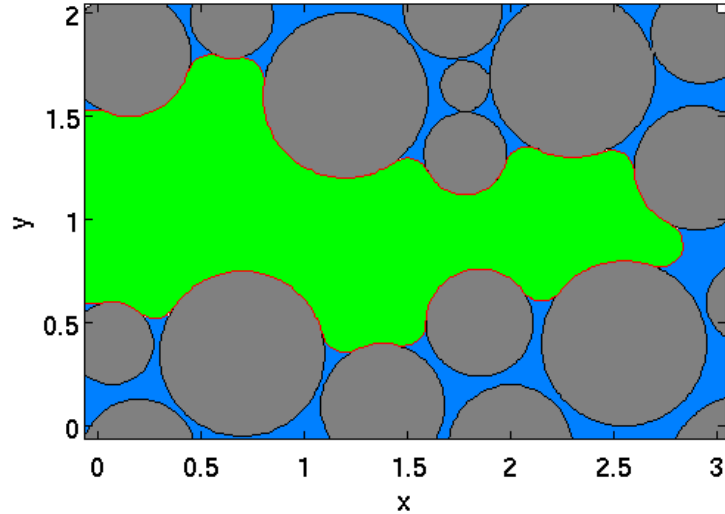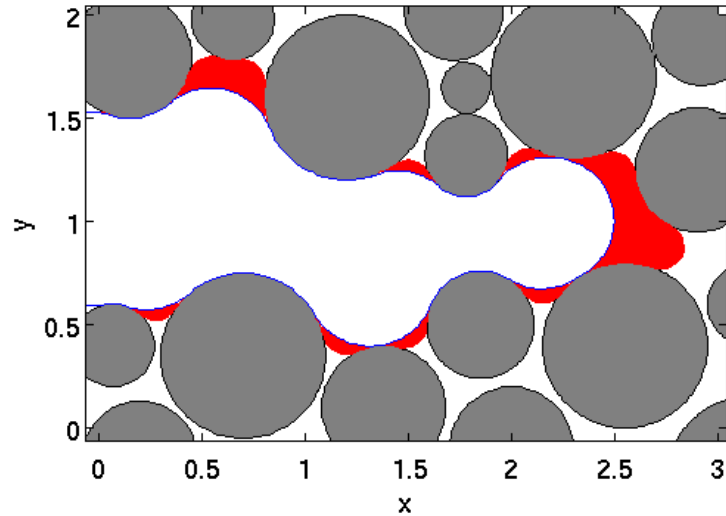

B. Stage 1, the incremental movements of gas/water interface due to hydrate formation (arrows from the red to blue interfaces; phases are not shown). This figure shows three sequential representative locations of interfaces during hydrate formation. The arrows indicate the directions that the interface moves and in which hydrate grows. The first layer of hydrate will form at the interface. Subsequent hydrate continues to grow into the gaseous phase.
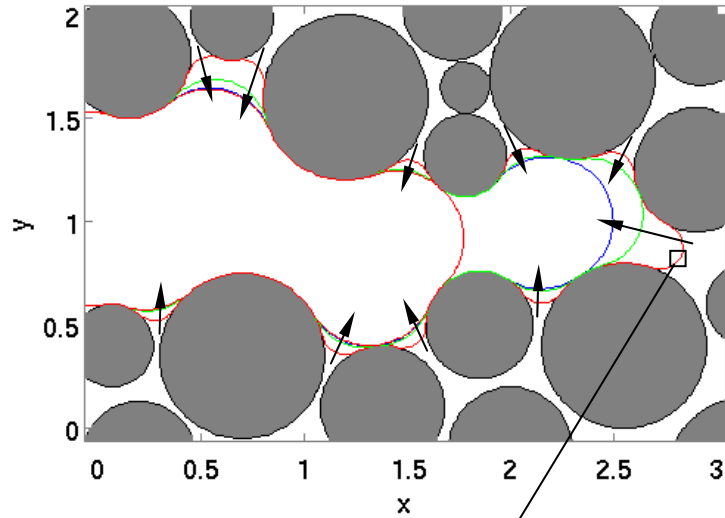
A schematic (inset and zoom below main figure) describes the mechanism by which water is supplied to maintain hydrate formation at the interface between gas and hydrate. Numerous tortuous conduits (blue) exist in the hydrate layer (red) since hydrate is porous. Water (blue) can therefore be sucked through the layer and coats the hydrate surface (for the water flow rate please see Appendix A). When in contact with gas (green), new hydrate can form at the gas-water interface. This is the driving mechanism for hydrate "invasion" of the gas-occupied pores.

water film

microporous
hydrate layer
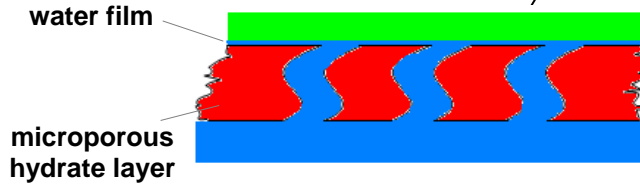
C. Hydrate distribution (red) when the interface (blue curve) is at the critical point (blue curve).

D. Stage 2, the incremental movement of gas-water interface (from blue to red interfaces; phases are not shown). The red curve is the capillary-stable curve if imbibition jump happens. But because of the limiting water supply, gradual incremental movement between blue and red curves happens during this stage. The rapid formation of hydrate means that similar to B, hydrate grows from the water film on the gas-hydrate interface and gradually invades the gaseous phase.
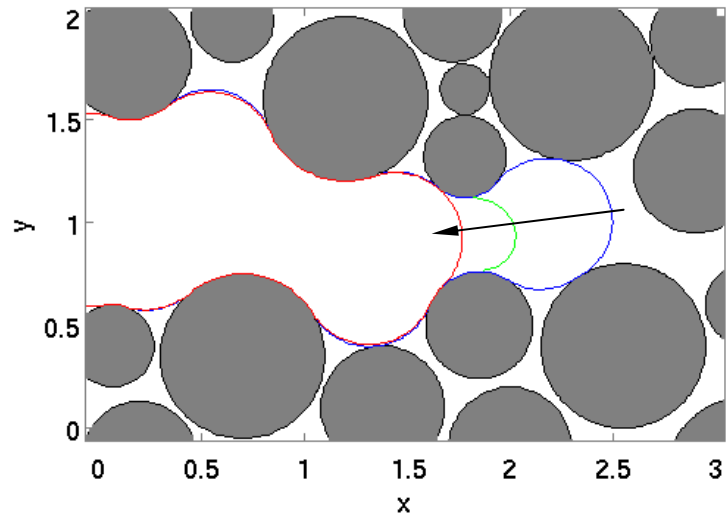
E. Hydrate distribution (red region) after stage 2. The total hydrate distribution is due to the hydrate formations in stages 1 and 2 (two stages are separated by the blue curve). Hydrate occupies the entire space that was taken up by gas before. That is, hydrate distribution replaces the initial gas distribution.

19
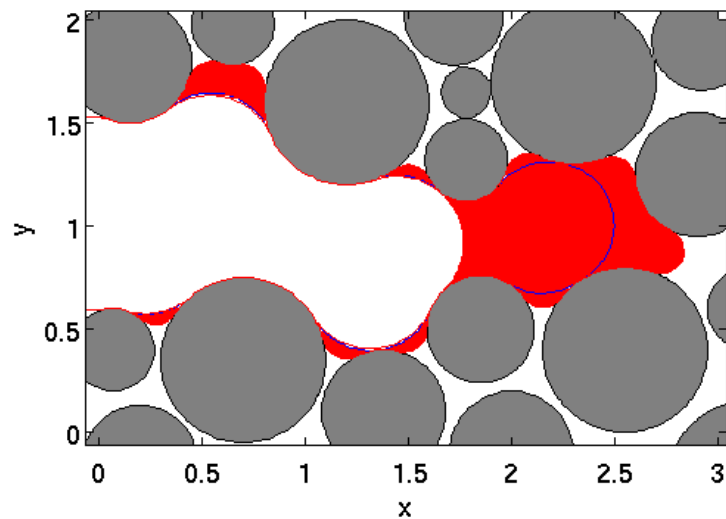
F. Stage 1 and 2 repeat themselves cyclically, which allows the hydrate formation slowly invades the gaseous phase. The final hydrate distribution from the right figure (red is hydrate and blue is water) is identical with the initial gas distribution in A.
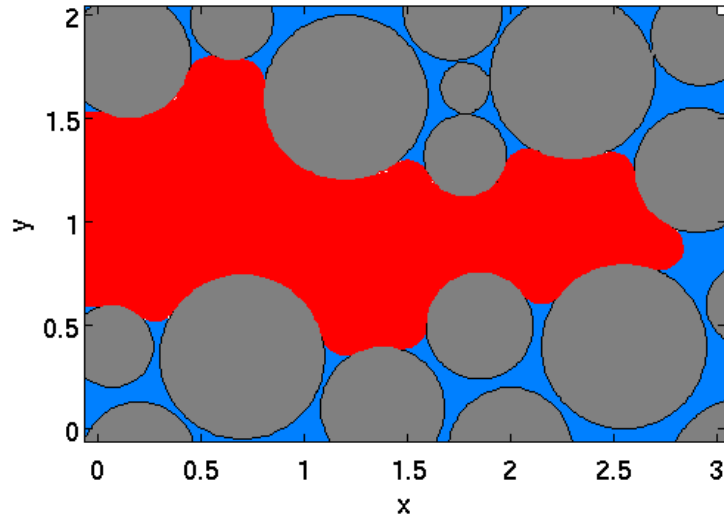

Figure 13. Schematics of limiting case #1, which gives the maximal hydrate saturation. The colors of interfaces are used for the identification purposes, and they are not associated with the phase colors.

The critical feature of this limiting case is that the gas-hydrate interfaces will gradually advance into the gas phase, so that adjacent interfaces eventually merge. This also means that separated gas-water interfaces merge as well, as water always coats the hydrate surface (Figure 13B the zoom-in figure) because of capillarity. We have previously established that the point of merger of gas/water interfaces is unstable: in classical imbibition, the interface will jump to a new location. This is the Melrose condition for imbibing a pore. However when two gas/hydrate interfaces (also gas/water interfaces) merge, a spontaneous Melrose imbibition event is not possible, because the fluid (water) is converted to a solid (hydrate) as soon as it reaches the gas-hydrate interface, and thus no extra water can be used for the imbibition jump. In other words, the limiting water supply disables imbibition events, and only the slow and incremental movement of interface is allowed (Figure 13D and E). This increment movement gives a similar pattern as for Figure 13B and 13C. That is, water is sucked through the hydrate layer and coats the hydrate surface as a thin layer, which is later converted into hydrate. This gradual movement of hydrate finally allows the interface to move into the following pores. We refer to this (Figure 13D and 13E) as stage 2.

This incremental motion has an important implication: all the gas phase initially present is eventually converted to hydrate. Thus the final hydrate saturation has the same pore-scale "footprint" (occupies the same pores, throats, etc.) as the initial gas saturation.

These two stages have the same behavior but driven by different forces. Stage 1 is controlled by the capillary equilibrium, which is independent of the water supply rate. Stage 2, which would exhibit an imbibition jump if both phases at the interface were fluids, happens only because the water supply rate is slower than the rate of hydrate formation at the gas/hydrate interface. These two stages happen cyclically.

This model allows for maximal hydrate saturation in the porous medium. Based on the assumption that hydrate grows into gaseous phase only, hydrate distribution fully repeat the footprint of the initial gas distribution (Figure 13F). The hydrate saturation is equal to the initial gas saturation.

We remark that the magnitude of the rate of water supply can be estimated, as discussed in Appendix A. The appropriate rate of hydrate formation remains to be determined, however.

**Limiting case #2: water supply rate much larger than hydrate formation rate**

This case has the same stage 1 as Limiting Case #1: hydrate slowly invades the gaseous phase (Figure 14B and C). When the gas-water interface reaches the critical point at which two interfaces merge (which is the end of stage 1), the fluid behavior becomes different. The assumption that water supply rate is much larger than the hydrate formation rate indicates that water supply is no longer a constraint for imbibition. At the critical point, therefore, a Melrose imbibition jump takes place due to the unstable fluid-fluid interface. This is the conventional imbibition process, and can be modeled by LSMPQS technique.

In Figure 14C, imbibition jump of a gas-brine interface takes place instead of the incremental movement. Consequently a large portion of the pore(s) will be filled by water. After the imbibition jump, a stable interface exists between gas and brine. As stated by the assumption, hydrate grows only into the gaseous phase. Therefore, water invasion during the imbibition jump will not be converted into hydrate (Figure 14D and E). Hydrate resumes growth only on the new stable locations of the gas/water interface(s), and into the gaseous phase as before. After several steps of incremental movement of the gas/hydrate interface into the gaseous phase, a Melrose imbibition jump happens again. This sequence of events leads to a sandwich-like pattern, illustrated at the

imbibition endpoint in Figure 14F: water droplets are encaged by hydrate shells in the entire porous medium.

It follows that this limiting case yields the minimal hydrate saturation. The original footprint of the gas phase is now occupied by water-filled pores and hydrate lenses of varying thickness. Since the water-filled pores are surrounded by hydrate shells, it is likely that the electrical resistivity of the final distribution of phases is quite similar to the resistivity of the final distribution of phases in Limiting Case #1. This has dramatic consequences for the interpretation of hydrate saturation from conventional correlations.

A. The initial methane (green) and water (blue) distribution in a porous medium (gray disks represent the sand grains). The distribution is in capillary equilibrium (satisfies Young-Laplace equation), obtained from the drainage endpoint by the LSMPQS simulation.
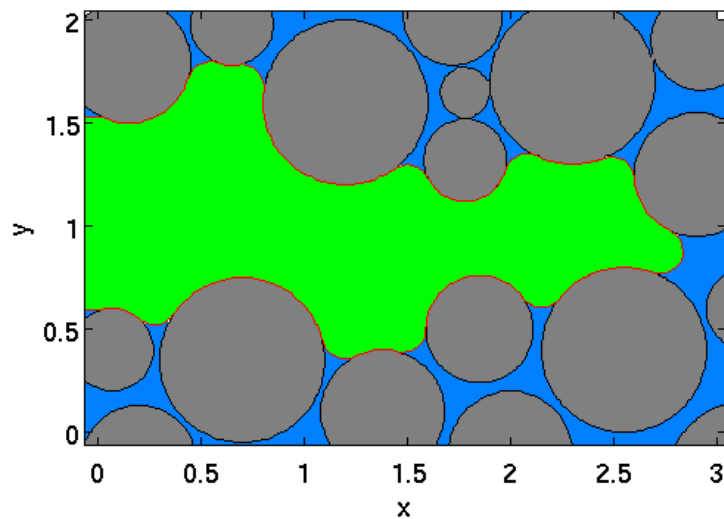
B. Stage 1, the incremental movements of interface due to hydrate formation (from the red to blue interfaces). This stage is the same as in Limiting Case #1, in Figure 13B.
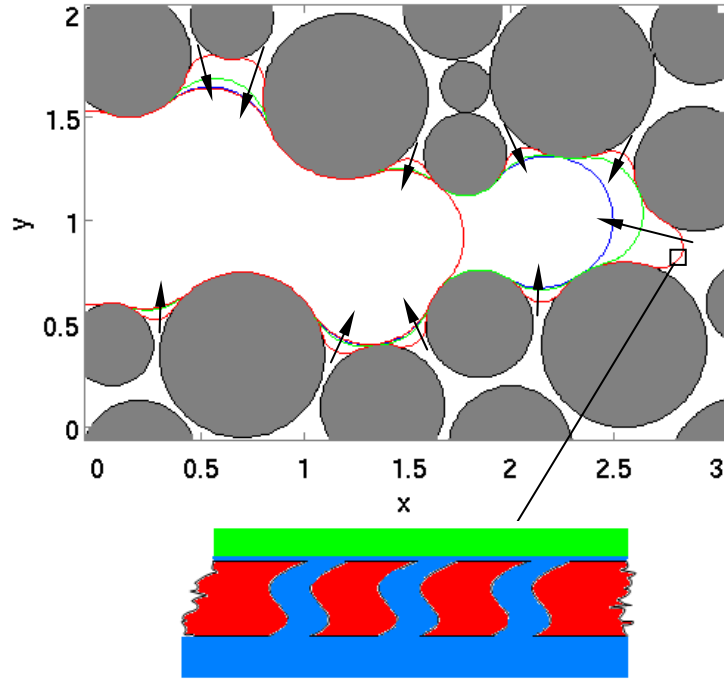

C. Hydrate distribution (red) when the gas-hydrate interface (blue curve) is at the critical point. Following this step, a slight decrement of curvature will result in a jump of interface to the left (Melrose imbibition jump). This is because the water film at the surface of the hydrate merges to form a single gas/water interface, which is unstable.
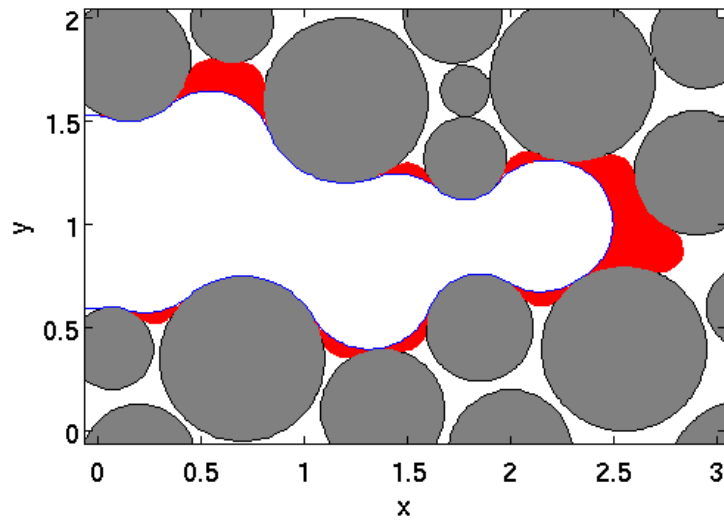
D. Stage 2, the imbibition jump is an abrupt, instantaneous process. No intermediate steps, like the green interface in Figure 1314D, will be available. Thus the interface jumps to the next stable position, which is shown as the red curve.
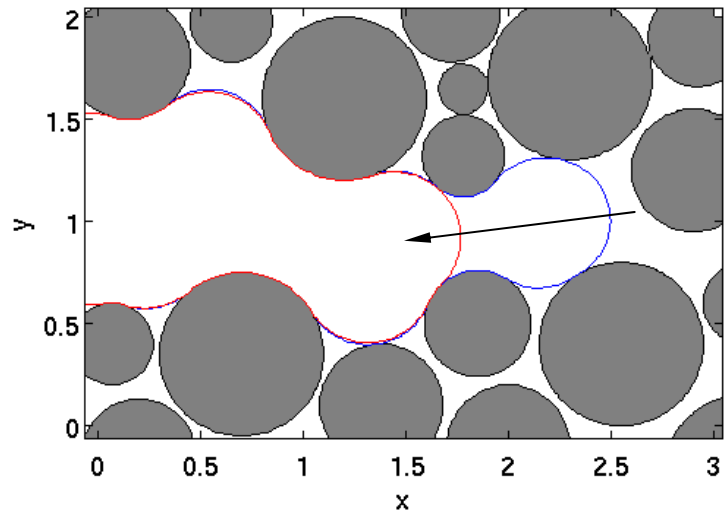
E. Imbibition jump sucks the water to fill the pore (blue). A new, stable location of the gas/water interface is reached at the end of the jump. New hydrate can from along the interface, and only grows into the gaseous phase (green). Thus the pore space taken up by water during the jump will not be converted into hydrate.
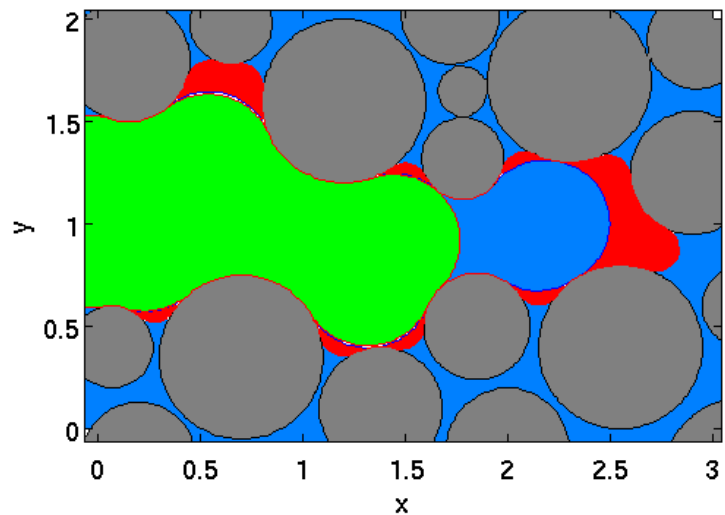
F. Stages 1 and 2 repeat themselves cyclically. We only show here the final hydrate (red) and water (blue) distribution. The final distribution has a sandwich-like pattern, which water-filled pores are separated by hydrate shells of varying thickness. This gives the minimal hydrate saturation.
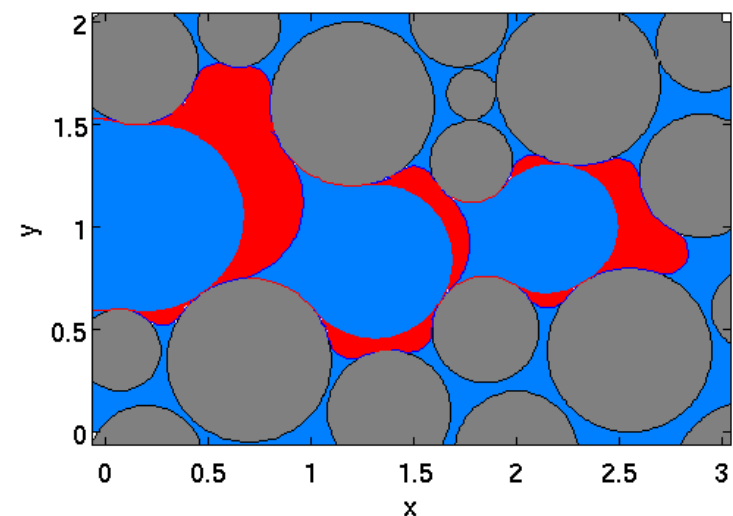

Figure 14. Schematics of limiting case #2, the color scheme is the same as in Figure 13. The colors of interfaces are used for the identification purposes, and they are not associated with the phase colors.

Relationship to Macroscopic Volume Change Model

It is conceptually straightforward (though complicated to implement) to compute the total amount of water that enters the domain in each of the limiting cases above. Likewise it is straightforward to compute the final hydrate saturation. Moreover as a reasonable first order approximation of the natural system, we can also assume that gas enters the domain in the stoichiometric quantity needed to yield the final hydrate saturation. (As discussed in previous reports, the needed gas would travel upwards from the accumulation below the BGHSZ.) Thus the two limiting cases above yield *a priori* estimates of the ratio of phase volumes (brine to gas) that enter the hydrate stability zone until the final hydrate saturation is reached. *This is precisely the parameter needed to make the model of macroscopic volume changes described in the first section of the report a predictive tool.* Work to explore this capability is ongoing and will be the subject of future reports.

Appendix A.

This calculation aims to obtain a rough estimate of the possible water transportation rate through a layer of hydrate between a gas phase and a brine phase. The competition of this transport rate with the hydrate formation rate determines whether the hydrate formation is restricted by the water supply. The entire calculation is based on the reasonable assumptions of the property values. We do not intend to give the accurate calculations; only the magnitudes are of interest here.

The calculation is based on a simple model (Figure 15).
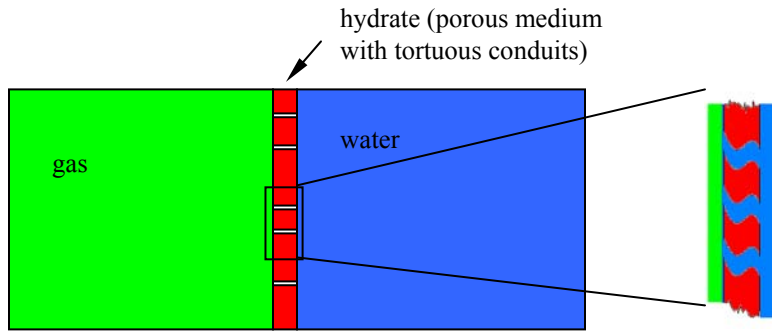

Figure 15. A schematic of the model. Gas and water phases are separated by the hydrate layer. Due to the imperfect nature of boundaries between crystalline regions of hydrate, numerous small and highly tortuous tubes exist in the hydrate layer. Water is transported through these conduits due to the pressure difference in gas and water.

We assume a porous medium with uniform grain radius of 100 microns. The pore radius is assumed to be 1/3~1/2 of the grain radius. In this calculation we use the upper bound, 50 microns. The throat radius is roughly 1/3 of the grain radius, and thus 33 microns. The defects in the hydrate layer are treated as capillary tubes that are conduits for water transportation. The radius of each conduit is set to be 1/20 of the throat size. These properties are listed below.

Properties	Values	Units	comments
Grain radius	100	Microns	
Pore radius	50	Microns	1/3~1/2 of grain radius
Pore volume	5.24e5	Microns^3	
Throat radius	33	Microns	1/3~1/4 of grain radius
Tube radius	1.6	Microns	1/20 of throat radius
Hydrate layer thickness	500	Microns	
Pressure difference	10	Psi	
Water viscosity	0.00166	Pa s	

Based on the above settings, Hagen-Poiseuille equation is used. We obtain the flow rate due to a single tube is $Q = 2\times10^5$ microns^3/s. This indicates that it takes less than 3 seconds for water to fill a pore (the pore volume, as listed above, is 5×10^5 microns^3). Therefore, it is possible for imbibition jump to take place even though with the presence of hydrate layer.

Of course the properties we use might be subject to large error. Based on a large range of properties we choose, we believe that both imbibition jump and incremental movement are possible in this hydrate-water-gas system. Therefore, it is important to know the upper and lower limits for hydrate saturation, as shown in the Limiting Case 1 and 2.

National Energy Technology Laboratory

626 Cochrans Mill Road
P.O. Box 10940
Pittsburgh, PA 15236-0940

3610 Collins Ferry Road
P.O. Box 880
Morgantown, WV 26507-0880

13131 Dairy Ashford, Suite 225
Sugarland, TX 77478

1450 Queen Avenue SW
Albany, OR 97321-2198

2175 University Ave. South
Suite 201
Fairbanks, AK 99709

Visit the NETL website at:
www.netl.doe.gov

Customer Service:
1-800-553-7681